Necroptosis of neuronal cells is related to the neuropathology of tick-borne encephalitis

Dai Tsujino[1], Kentaro Yoshii[1, 2]*, Misa Kajiyama[1], Yuji Takahashi[1], Naoya Maekawa[3], Hiroaki Kariwa[1], and Shintaro Kobayashi[1]*

[1]Laboratory of Public Health, Faculty of Veterinary Medicine, Hokkaido University, Sapporo, Japan
[2]National Research Center for the Control and Prevention of Infectious Diseases (CCPID), Nagasaki University, Nagasaki, Japan
[3]Department of Advanced Pharmaceutics, Faculty of Veterinary Medicine, Hokkaido University, Sapporo, Japan

*Co-Corresponding author
Shintaro Kobayashi
E-mail: shin-kobayashi@vetmed.hokudai.ac.jp
Kentaro Yoshii
E-mail: kyoshii@nagasaki-u.ac.jp

Keywords
tick-borne encephalitis virus, programmed cell death, necroptosis

Abstract

Tick-borne encephalitis virus (TBEV) is a zoonotic virus that causes tick-borne encephalitis (TBE) in humans. Infections of Sapporo-17-Io1 (Sapporo) and Oshima 5-10 (Oshima) TBEV strains showed different pathogenic effects in mice. However, the differences between the two strains are unknown. In this study, we examined neuronal degeneration and death, and activation of glial cells in mice inoculated with each strain to investigate the pathogenesis of TBE. Viral growth was similar between Sapporo and Oshima, but neuronal degeneration and death, and activation of glial cells, was more prominent with Oshima. In human neuroblastoma cells, apoptosis and pyroptosis were not observed after TBEV infection. However, the expression of the necroptosis marker, mixed lineage kinase domain-like (MLKL) protein, was upregulated by TBEV infection, and this upregulation was

more pronounced in Oshima than Sapporo infections. As necroptosis is a pro-inflammatory type of cell death, differences in necroptosis induction might be involved in the differences in neuropathogenicity of TBE.

Tick-borne encephalitis virus (TBEV), a member of the genus *Flavivirus* and the family *Flaviviridae*, causes tick-borne encephalitis (TBE) and long-term neurological sequelae (Gritsun et al., 2003). TBEV is prevalent throughout northern Eurasia, including Europe, Russia, Far East Asia, and Japan (Gritsun et al., 2003; Takahashi et al., 2020; Takashima et al., 1997). The global incidence of TBE exceeds 10,000 patients per year (Takahashi et al., 2020). TBEV causes central nervous system (CNS) infection with clinical manifestations ranging from mild biphasic fever to severe encephalitis and meningoencephalitis (Dumpis et al., 1999; Ecker et al., 1999). It has a mortality rate of 0.5–30% (Gritsun et al., 2003). Although there are several effective vaccines, there is no specific therapeutic treatment for TBE (Andersson et al., 2010; Morozova et al., 2014; Petry et al., 2021).

TBEV is primarily transmitted to humans by the *Ixodes* sp., but is also occasionally acquired by the consumption of unpasteurized dairy products from infected livestock (Balogh et al., 2010; Brockmann et al., 2018). The virus causes encephalitis, along with neuronal cell degeneration and death, glial cell activation, and immune cell infiltration (Pokorna Formanova et al., 2019). TBEV mainly targets the CNS and causes neuronal cell death through two pathways: direct induction of programmed cell death or neuronal injury through an uncontrolled inflammatory response involving glial cytokines and chemokines (Hayasaka et al., 2009; Ruzek et al., 2009a; Ye et al., 2013). However, the details of these pathways and underlying molecular mechanisms are still largely unknown.

Programmed cell death, including apoptosis, pyroptosis, and necroptosis, plays a vital role in maintaining homeostasis, and in anti-viral responses (Okamoto et al., 2017; Wen et al., 2021). Apoptosis is tightly controlled cell death designed to avoid inflammation (Fricker et al., 2018; Galluzzi et al., 2018). Pyroptosis and necroptosis, which are programmed forms of necrosis, cause membrane disruption and allow the release of pro-inflammatory and immunogenic cellular contents (Frank and Vince, 2019; Fricker et al., 2018; Galluzzi et al., 2018; McKenzie et al., 2020; Mocarski et al., 2015; Vanden Berghe et al., 2014). It has been reported that TBEV infection triggers apoptosis and pyroptosis, while other flavivirus infection, such as West Nile virus or Japanese encephalitis virus infection, induces apoptosis, pyroptosis, and necroptosis (Bian et al., 2017; Cheung et al., 2018; Fares et al., 2020; Fares et al., 2021; He et al., 2020; Kobayashi et al., 2012; Lim et al., 2017; Okamoto et al., 2017; Ruzek et al., 2009b; Wang et al., 2020; Wen et al., 2021). It is important to elucidate the relationship between programmed cell death and TBEV infection to understand the neuropathogenesis of TBE.

We previously reported differences in pathogenicity among TBEV strains with high homology (Takahashi et al., 2020), which is important for understanding TBE pathogenesis. Therefore, in this study, we performed histopathological analysis of mouse brains infected with different strains, and found differences in neuronal degeneration and death, as well as glial activation. We found that the induction of necroptosis in cultured cells was different between the two strains.

Recombinant TBEV Oshima 5-10 and Sapporo-17-Io1 strains (GenBank accession nos. AB062063.2 and LC440459.1, respectively) (Takahashi et al., 2020; Takashima et al., 1997), which belong to different sub-clusters of the Far-eastern subtype, were recovered from infectious cDNA clones as previously described (Takano et al., 2011; Takashima et al., 1997). Working stocks of the virus were

propagated once in BHK-21 cells. Experiments using live TBEV were conducted in Biosafety Level 3 (BSL-3) facilities located at the Graduate School of Veterinary Medicine, Hokkaido University.

The mice were intracerebrally inoculated with TBEV using a previously described method (Takahashi et al., 2020). Either 10 µL of virus stock containing 50 plaque forming units (pfu) of TBEV or the same volume of PBS was injected intracerebrally into female BALB/c mice (5 weeks old; Japan SLC, Shizuoka, Japan). All animal experiments were performed at the Animal Biosafety Level 3 (ABSL-3) facility of the Graduate School of Veterinary Medicine, Hokkaido University in accordance with institutional guidelines. Ethical approval was obtained from the Hokkaido University Animal Care and Use Committee (19-0142). The mice were sacrificed at 1, 4, or 7 days post inoculation (dpi), and viral titers in the brain were measured using plaque assays, as described previously (Takahashi et al., 2020). The virus was not detected in the brains at 1 dpi and the viral titers were similar between brains inoculated with the Sapporo and Oshima strains at both 4 and 7 dpi (Fig. 1a). The left brains' halves of TBEV-inoculated mice were collected in formalin, fixed, and then embedded in paraffin. The sections were stained with hematoxylin and eosin for histopathological analysis. For immunohistochemical (IHC) analysis, the sections were subjected to antigen retrieval using a pressure cooker in the presence of 10 mM sodium citrate buffer. The histopathological analysis of inoculated brains showed cell shrinkage and neuronophagia in regions close to the TBEV-antigen-positive cells in the cerebral cortices (Fig. 1b). Although the number of viral antigen-positive cells was almost the same, cell shrinkage was more frequent in Oshima- compared to Sapporo-inoculated mice (Fig. 1b). This suggested that mice infected with the Oshima strain were more susceptible to cell degeneration and death. As the viral growth properties of the two strains were not different, the difference in cell degeneration and death was not related to viral growth.

Next, we analysed the morphologies of TBEV-infected neurons. It has been reported that a decrease in fluorescence intensity of neuronal cell markers and cell shrinkage are associated with neuronal cell degeneration and death (Clarke et al., 2021). The neurons were visualized using the Alexa Fluor 647 Anti-MAP2 antibody (Abcam, Cambridge, UK) and evaluated for cell morphology and fluorescence intensity using ZEN 3.1.0 software (Carl Zeiss AG, Oberkochen, Germany). Based on a previous study, MAP2-positive cells in PBS-inoculated mice were used as controls to obtain the morphological scores of TBEV-inoculated mice (range: 1–4; 1, severe shrinkage; 2, moderate shrinkage; 3, mild shrinkage; 4, almost the same as control) (Petry et al., 2021). Fluorescence intensity and morphological scores were lower in viral antigen-positive cells compared to controls, and the reduction was more marked in Oshima-inoculated cells (Fig. 1c–e). This suggested that Oshima inoculation induced a greater degree of neuronal cell degeneration and death than Sapporo inoculation.

Astrocytes and microglia contribute to immunity and inflammation in the CNS (Barres, 2008; Nayak et al., 2014; Nedergaard et al., 2003; Sofroniew and Vinters, 2010). We examined the activation of astrocytes and microglia after inoculation with each strain to determine the differences in encephalitis caused by Sapporo and Oshima infections. We counted the number of glial fibrillary acidic protein (GFAP, astrocyte marker)-positive cells and ionized calcium-binding adapter molecule 1 (Iba-1, microglia marker)-positive cells in the cerebral cortices in five fields of three different mice, inoculated with TBEV or PBS. The number of GFAP- and Iba-1-positive cells was greater in TBEV- compared to PBS-inoculated mice (Fig. 2a, b, d, and e). The increase was more marked in Oshima- than Sapporo-inoculated cells (Fig. 2b and e). As astrocyte hypertrophy implies activation (Sticozzi et al., 2013; Zhou et al., 2001), the area of GFAP-positive cells in the cerebral cortices of

TBEV-inoculated mice was measured and compared to that of PBS mice using ImageJ software (https://imagej.nih.gov/ij/index.html). The size of GFAP-positive cells in Oshima-inoculated brains was larger compared to Sapporo-inoculated brains (Fig. 2c). Activated microglia have an amoeboid morphology, with larger cell bodies and fewer dendrites compared to normal microglia (Nayak et al., 2014; Subhramanyam et al., 2019). We counted the Iba-1-positive amoeboid cells. Few amoeboid Iba-1-positive cells were observed in PBS-inoculated brains. However, the number of these cells was increased significantly in Oshima- compared to Sapporo-inoculated brains (Fig. 2f). This suggested that the Oshima strain induced more neuroinflammation than the Sapporo strain.

We previously reported that Oshima infection was more pathogenic for mice than Sapporo infection (Takahashi et al., 2020). It was suggested that the neuropathogenesis of TBEV infection in mice was associated with neuronal cell death and neuroinflammation.

It is known that the type of cell death affects the induction of inflammation (Frank and Vince, 2019; Mocarski et al., 2015). Differences in the degeneration and death of neuronal cells, and inflammatory responses, in the brain were observed between Sapporo and Oshima infections. Therefore, we analysed the types of programmed cell death caused by each TBEV strain. Human neuroblastoma SH-SY5Y cells were inoculated with Sapporo or Oshima at a multiplicity of infection of 1, and then stained with propidium iodide (PI) to explore the extents to which the TBEVs induce cell death. Few PI-positive cells were detected at 24 hpi (Fig. 3a). The PI-positive rate was significantly higher in the cells infected with TBEV as compared to control cells and the increase was more evident in Oshima-infected cells than in Sapporo-infected cells at 48 hpi (Fig. 3a). At 72 hpi, many control cells were PI-positive; the PI-positive proportion of TBEV-infected cells was higher than that of control cells (Fig. 3a). TBEV-infected SH-SY5Y cells were lysed at 48 hpi in RIPA buffer (150 mM NaCl, 1% Triton X-100, 0.1% SDS, 0.5% sodium deoxycholate, 50 mM Tris;

pH 8.0) with a protease inhibitor (Nacalai Tesque, Kyoto, Japan) and phosphatase inhibitor cocktail 2 and 3 (Sigma-Aldrich, St. Louis, MO, USA). The expression of the apoptosis marker, cleaved-caspase 3, was undetectable in the cells infected with TBEV (Fig. 3b). Then, we examined caspase 1 and gasdermin D (GSDMD), which are markers of pyroptosis, and no difference was observed between control and TBEV-inoculated cells (Fig. 3c). Next, the expression levels of mixed lineage kinase domain-like (MLKL), phosphorylated MLKL (p-MLKL), RIP, and RIP3 were examined; these proteins are markers of necroptosis. The MLKL, p-MLKL, and RIP3 levels were increased by TBEV inoculation, and the increase was greater in Oshima- than Sapporo-infected cells (Fig. 3d and e). Subtle RIP upregulation was observed in TBEV-inoculated cells as compared to control; a greater increase was apparent in Oshima-inoculated cells (Fig. 3d). Addition of a necroptosis inhibitor (necrostatin-1s; Cell Signaling Technology, Beverly, MA, USA), decreased the PI-positive proportion of TBEV-infected cells (Fig. 3f). Furthermore, MLKL-positive cells were found in mouse brains inoculated with the Oshima (Fig. 3g). These results suggested that necroptosis, and not apoptosis or pyroptosis, was induced by TBEV infection, and that Oshima infection induced necroptosis more strongly than Sapporo infection.

In this study, we found that the incidence rates of neuronal degeneration and death, and inflammation with glial activation, differed between TBEV strains. Furthermore, the occurrence of necroptosis also differed between strains. TBEV strains more pathogenic for mice induced necroptosis more strongly than stains with lower pathogenicity. This suggested that necroptosis was important for its neuropathogenesis.

Since cytopathic effects and morphological characteristics of cell death were observed in TBEV-infected cultured cells, it appears that TBEV infection directly induces neuronal cell death (Gelpi et

al., 2005). However, previous studies demonstrated that excessive immune responses were induced by TBEV and other flaviviruses, which may cause neuronal cell death (Ghoshal et al., 2007; Hayasaka et al., 2009; Luo et al., 2018; Ruzek et al., 2009a). In this study, we demonstrated that necroptosis was induced in cultured human neuroblastoma cells infected with TBEV, suggesting that TBEV infection could induce necroptosis of neuronal cells without any influence of external factors. In the neuropathogenesis of TBE, viral infection induces necroptosis directly, and necroptosis might then activate glial cells, leading to encephalitis.

Elucidation of its neuropathogenesis may lead to the development of effective therapies for TBEV infection. Comparison of the two TBEV strains with high amino acid homology may lead to the elucidation of molecular mechanisms of necroptosis induced by TBEV, and aid identification of potential therapeutic targets for TBE.

Author statements

Authors and contributions

D.T.: validation, formal analysis, investigation, data curation, write – original draft preparation, visualization. K.Y.: write – review and editing, supervision, funding. M.K.: validation, formal analysis, investigation, data curation. Y.T.: resources, write – review and editing. N.M.: investigation, data curation. H.K.: resources, write – review and editing. S.K.: conceptualization, methodology, resources, write – review and editing, supervision, funding.

Conflicts of interest

The authors declare that there are no conflicts of interest.

Funding information

This work was supported in part by the Japan Society for the Promotion of Science (JSPS) KAKENHI Grant Numbers, 18K14574, 20K06406, 17H03910, 19K22353, 20H03136 and 21KK0123; the Research Program on Emerging and Re-emerging Infectious Diseases from Japan Agency for Medical Research and Development, AMED (21fk0108614h0301, JP21fk0108567h0001); Takeda Science Foundation; Suhara Memorial Foundation; Kuribayashi Foundation; MSD Life Science Foundation, Public Interest Incorporated Foundation; The Akiyama Life Science Foundation ;Grant for Joint Research Program of the Institute for Genetic Medicine, Hokkaido University; Joint Usage / Research Center on Tropical Disease, Institute of Tropical Medicine, Nagasaki University (2021-Ippan-14); the World-leading Innovative and Smart Education (WISE) Program (1801) from the Ministry of Education, Culture, Sports, and Technology, Japan.

Ethical approval

All animal experiments were performed following the basic guidelines for animal experiments of the Ministry of Education, Culture, Sports, Science and Technology (MEXT), Japan. The President of Hokkaido University approved all animal experiments after review by the Institutional Animal Care and Use Committee of Hokkaido University (approval no. 19-0142).

References

Andersson, C.R., Vene, S., Insulander, M., Lindquist, L., Lundkvist, A., Gunther, G., 2010. Vaccine failures after active immunisation against tick-borne encephalitis. Vaccine 28(16), 2827-2831.

Balogh, Z., Ferenczi, E., Szeles, K., Stefanoff, P., Gut, W., Szomor, K.N., Takacs, M., Berencsi, G., 2010. Tick-borne encephalitis outbreak in Hungary due to consumption of raw goat milk. J Virol Methods 163(2), 481-485.

Barres, B.A., 2008. The mystery and magic of glia: a perspective on their roles in health and disease. Neuron 60(3), 430-440.

Bian, P., Zheng, X., Wei, L., Ye, C., Fan, H., Cai, Y., Zhang, Y., Zhang, F., Jia, Z., Lei, Y., 2017. MLKL Mediated Necroptosis Accelerates JEV-Induced Neuroinflammation in Mice. Front Microbiol 8, 303.

Brockmann, S.O., Oehme, R., Buckenmaier, T., Beer, M., Jeffery-Smith, A., Spannenkrebs, M., Haag-Milz, S., Wagner-Wiening, C., Schlegel, C., Fritz, J., Zange, S., Bestehorn, M., Lindau, A., Hoffmann, D., Tiberi, S., Mackenstedt, U., Dobler, G., 2018. A cluster of two human cases of tick-borne encephalitis (TBE) transmitted by unpasteurised goat milk and cheese in Germany, May 2016. Euro Surveill 23(15).

Cheung, K.T., Sze, D.M., Chan, K.H., Leung, P.H., 2018. Involvement of caspase-4 in IL-1 beta production and pyroptosis in human macrophages during dengue virus infection. Immunobiology 223(4-5), 356-364.

Clarke, P., Leser, J.S., Tyler, K.L., 2021. Intrinsic Innate Immune Responses Control Viral Growth and Protect against Neuronal Death in an Ex Vivo Model of West Nile Virus-Induced Central Nervous System Disease. J Virol 95(18), e0083521.

Dumpis, U., Crook, D., Oksi, J., 1999. Tick-borne encephalitis. Clin Infect Dis 28(4), 882-890.

Ecker, M., Allison, S.L., Meixner, T., Heinz, F.X., 1999. Sequence analysis and genetic classification of tick-borne encephalitis viruses from Europe and Asia. The Journal of general virology 80 (Pt 1), 179-185.

Fares, M., Cochet-Bernoin, M., Gonzalez, G., Montero-Menei, C.N., Blanchet, O., Benchoua, A., Boissart, C., Lecollinet, S., Richardson, J., Haddad, N., Coulpier, M., 2020. Pathological modeling of TBEV infection reveals differential innate immune responses in human neurons and astrocytes that correlate with their susceptibility to infection. J Neuroinflammation 17(1), 76.

Fares, M., Gorna, K., Berry, N., Cochet-Bernoin, M., Piumi, F., Blanchet, O., Haddad, N., Richardson, J., Coulpier, M., 2021. Transcriptomic Studies Suggest a Coincident Role for Apoptosis and Pyroptosis but Not for Autophagic Neuronal Death in TBEV-Infected Human Neuronal/Glial Cells. Viruses 13(11).

Frank, D., Vince, J.E., 2019. Pyroptosis versus necroptosis: similarities, differences, and crosstalk. Cell Death Differ 26(1), 99-114.

Fricker, M., Tolkovsky, A.M., Borutaite, V., Coleman, M., Brown, G.C., 2018. Neuronal Cell Death. Physiol Rev 98(2), 813-880.

Galluzzi, L., Vitale, I., Aaronson, S.A., Abrams, J.M., Adam, D., Agostinis, P., Alnemri, E.S., Altucci, L., Amelio, I., Andrews, D.W., Annicchiarico-Petruzzelli, M., Antonov, A.V., Arama, E., Baehrecke, E.H., Barlev, N.A., Bazan, N.G., Bernassola, F., Bertrand, M.J.M., Bianchi, K., Blagosklonny, M.V., Blomgren, K., Borner, C., Boya, P., Brenner, C., Campanella, M., Candi, E., Carmona-Gutierrez, D., Cecconi, F., Chan, F.K., Chandel, N.S.,

Cheng, E.H., Chipuk, J.E., Cidlowski, J.A., Ciechanover, A., Cohen, G.M., Conrad, M., Cubillos-Ruiz, J.R., Czabotar, P.E., D'Angiolella, V., Dawson, T.M., Dawson, V.L., De Laurenzi, V., De Maria, R., Debatin, K.M., DeBerardinis, R.J., Deshmukh, M., Di Daniele, N., Di Virgilio, F., Dixit, V.M., Dixon, S.J., Duckett, C.S., Dynlacht, B.D., El-Deiry, W.S., Elrod, J.W., Fimia, G.M., Fulda, S., Garcia-Saez, A.J., Garg, A.D., Garrido, C., Gavathiotis, E., Golstein, P., Gottlieb, E., Green, D.R., Greene, L.A., Gronemeyer, H., Gross, A., Hajnoczky, G., Hardwick, J.M., Harris, I.S., Hengartner, M.O., Hetz, C., Ichijo, H., Jaattela, M., Joseph, B., Jost, P.J., Juin, P.P., Kaiser, W.J., Karin, M., Kaufmann, T., Kepp, O., Kimchi, A., Kitsis, R.N., Klionsky, D.J., Knight, R.A., Kumar, S., Lee, S.W., Lemasters, J.J., Levine, B., Linkermann, A., Lipton, S.A., Lockshin, R.A., Lopez-Otin, C., Lowe, S.W., Luedde, T., Lugli, E., MacFarlane, M., Madeo, F., Malewicz, M., Malorni, W., Manic, G., et al., 2018. Molecular mechanisms of cell death: recommendations of the Nomenclature Committee on Cell Death 2018. Cell Death Differ 25(3), 486-541.

Gelpi, E., Preusser, M., Garzuly, F., Holzmann, H., Heinz, F.X., Budka, H., 2005. Visualization of Central European tick-borne encephalitis infection in fatal human cases. J Neuropathol Exp Neurol 64(6), 506-512.

Ghoshal, A., Das, S., Ghosh, S., Mishra, M.K., Sharma, V., Koli, P., Sen, E., Basu, A., 2007. Proinflammatory mediators released by activated microglia induces neuronal death in Japanese encephalitis. Glia 55(5), 483-496.

Gritsun, T.S., Lashkevich, V.A., Gould, E.A., 2003. Tick-borne encephalitis. Antiviral Res 57(1-2), 129-146.

Hayasaka, D., Nagata, N., Fujii, Y., Hasegawa, H., Sata, T., Suzuki, R., Gould, E.A., Takashima, I., Koike, S., 2009. Mortality following peripheral infection with tick-borne encephalitis virus results from a combination of central nervous system pathology, systemic inflammatory and stress responses. Virology 390(1), 139-150.

He, Z., An, S., Chen, J., Zhang, S., Tan, C., Yu, J., Ye, H., Wu, Y., Yuan, J., Wu, J., Zhu, X., Li, M., 2020. Neural progenitor cell pyroptosis contributes to Zika virus-induced brain atrophy and represents a therapeutic target. Proc Natl Acad Sci U S A 117(38), 23869-23878.

Kobayashi, S., Orba, Y., Yamaguchi, H., Kimura, T., Sawa, H., 2012. Accumulation of ubiquitinated proteins is related to West Nile virus-induced neuronal apoptosis. Neuropathology 32(4), 398-405.

Lim, S.M., van den Ham, H.J., Oduber, M., Martina, E., Zaaraoui-Boutahar, F., Roose, J.M., van, I.W.F.J., Osterhaus, A., Andeweg, A.C., Koraka, P., Martina, B.E.E., 2017. Transcriptomic Analyses Reveal Differential Gene Expression of Immune and Cell Death Pathways in the Brains of Mice Infected with West Nile Virus and Chikungunya Virus. Front Microbiol 8, 1556.

Luo, H., Winkelmann, E.R., Zhu, S., Ru, W., Mays, E., Silvas, J.A., Vollmer, L.L., Gao, J., Peng, B.H., Bopp, N.E., Cromer, C., Shan, C., Xie, G., Li, G., Tesh, R., Popov, V.L., Shi, P.Y., Sun, S.C., Wu, P., Klein, R.S., Tang, S.J., Zhang, W., Aguilar, P.V., Wang, T., 2018. Peli1 facilitates virus replication and promotes neuroinflammation during West Nile virus infection. J Clin Invest 128(11), 4980-4991.

McKenzie, B.A., Dixit, V.M., Power, C., 2020. Fiery Cell Death: Pyroptosis in the Central Nervous System. Trends Neurosci 43(1), 55-73.

Mocarski, E.S., Guo, H., Kaiser, W.J., 2015. Necroptosis: The Trojan horse in cell autonomous antiviral host defense. Virology 479-480, 160-166.

Morozova, O.V., Bakhvalova, V.N., Potapova, O.F., Grishechkin, A.E., Isaeva, E.I., Aldarov, K.V., Klinov, D.V., Vorovich, M.F., 2014. Evaluation of immune response and protective effect of four vaccines against the tick-borne encephalitis virus. Vaccine 32(25), 3101-3106.

Nayak, D., Roth, T.L., McGavern, D.B., 2014. Microglia development and function. Annu Rev Immunol 32, 367-402.

Nedergaard, M., Ransom, B., Goldman, S.A., 2003. New roles for astrocytes: redefining the functional architecture of the brain. Trends Neurosci 26(10), 523-530.

Okamoto, T., Suzuki, T., Kusakabe, S., Tokunaga, M., Hirano, J., Miyata, Y., Matsuura, Y., 2017. Regulation of Apoptosis during Flavivirus Infection. Viruses 9(9).

Petry, M., Palus, M., Leitzen, E., Mitterreiter, J.G., Huang, B., Kroger, A., Verjans, G., Baumgartner, W., Rimmelzwaan, G.F., Ruzek, D., Osterhaus, A., Prajeeth, C.K., 2021. Immunity to TBEV Related Flaviviruses with Reduced Pathogenicity Protects Mice from Disease but Not from TBEV Entry into the CNS. Vaccines (Basel) 9(3).

Pokorna Formanova, P., Palus, M., Salat, J., Honig, V., Stefanik, M., Svoboda, P., Ruzek, D., 2019. Changes in cytokine and chemokine profiles in mouse serum and brain, and in human neural cells, upon tick-borne encephalitis virus infection. J Neuroinflammation 16(1), 205.

Ruzek, D., Salat, J., Palus, M., Gritsun, T.S., Gould, E.A., Dykova, I., Skallova, A., Jelinek, J., Kopecky, J., Grubhoffer, L., 2009a. CD8+ T-cells mediate immunopathology in tick-borne encephalitis. Virology 384(1), 1-6.

Ruzek, D., Vancova, M., Tesarova, M., Ahantarig, A., Kopecky, J., Grubhoffer, L., 2009b. Morphological changes in human neural cells following tick-borne encephalitis virus infection. The Journal of general virology 90(Pt 7), 1649-1658.

Sofroniew, M.V., Vinters, H.V., 2010. Astrocytes: biology and pathology. Acta Neuropathol 119(1), 7-35.

Sticozzi, C., Belmonte, G., Meini, A., Carbotti, P., Grasso, G., Palmi, M., 2013. IL-1beta induces GFAP expression in vitro and in vivo and protects neurons from traumatic injury-associated apoptosis in rat brain striatum via NFkappaB/Ca(2)(+)-calmodulin/ERK mitogen-activated

protein kinase signaling pathway. Neuroscience 252, 367-383.
Subhramanyam, C.S., Wang, C., Hu, Q., Dheen, S.T., 2019. Microglia-mediated neuroinflammation in neurodegenerative diseases. Semin Cell Dev Biol 94, 112-120.
Takahashi, Y., Kobayashi, S., Ishizuka, M., Hirano, M., Muto, M., Nishiyama, S., Kariwa, H., Yoshii, K., 2020. Characterization of tick-borne encephalitis virus isolated from a tick in central Hokkaido in 2017. The Journal of general virology 101(5), 497-509.
Takano, A., Yoshii, K., Omori-Urabe, Y., Yokozawa, K., Kariwa, H., Takashima, I., 2011. Construction of a replicon and an infectious cDNA clone of the Sofjin strain of the Far-Eastern subtype of tick-borne encephalitis virus. Archives of virology 156(11), 1931-1941.
Takashima, I., Morita, K., Chiba, M., Hayasaka, D., Sato, T., Takezawa, C., Igarashi, A., Kariwa, H., Yoshimatsu, K., Arikawa, J., Hashimoto, N., 1997. A case of tick-borne encephalitis in Japan and isolation of the the virus. J Clin Microbiol 35(8), 1943-1947.
Vanden Berghe, T., Linkermann, A., Jouan-Lanhouet, S., Walczak, H., Vandenabeele, P., 2014. Regulated necrosis: the expanding network of non-apoptotic cell death pathways. Nat Rev Mol Cell Biol 15(2), 135-147.
Wang, Z.Y., Zhen, Z.D., Fan, D.Y., Wang, P.G., An, J., 2020. Transcriptomic Analysis Suggests the M1 Polarization and Launch of Diverse Programmed Cell Death Pathways in Japanese Encephalitis Virus-Infected Macrophages. Viruses 12(3).
Wen, C., Yu, Y., Gao, C., Qi, X., Cardona, C.J., Xing, Z., 2021. RIPK3-Dependent Necroptosis Is Induced and Restricts Viral Replication in Human Astrocytes Infected With Zika Virus. Front Cell Infect Microbiol 11, 637710.
Ye, J., Zhu, B., Fu, Z.F., Chen, H., Cao, S., 2013. Immune evasion strategies of flaviviruses. Vaccine 31(3), 461-471.
Zhou, R., Wu, X., Skalli, O., 2001. TGF-alpha induces a stationary, radial-glia like phenotype in cultured astrocytes. Brain Res Bull 56(1), 37-42.

Figure legends

Fig. 1. Cell degeneration and death in mouse brains induced by TBEV infection. Oshima induced more cell degeneration and death than Sapporo.

(a) Virus titers in mouse brains were determined using plaque assay. The brains were weighted and homogenised (10% w/v suspension in PBS). The data are presented as mean ± SD. The Student's t

test revealed no significant differences between the two strains.

(b) The serial sections were stained by hematoxylin and eosin (upper panels). Immunohistochemistry was performed for the TBEV E-protein (lower panels). Arrows indicate representative degenerative cells. (c) Double staining with TBEV E-protein (green) and MAP2 (red). (d) Relative MAP2 fluorescence intensity was measured. MAP2 fluorescence intensity was measured in eight fields/mouse (n = 3 and n = 1; for Sapporo- and Oshima-inoculated mice, and a control mouse, respectively). The data are presented as mean + SD; Tukey-Kramer test, **p < 0.01. (e) Morphological score of TBEV-infected neurons. Scores were based on the size of the clear area around TBEV-positive neurons. Scores ranged from 1 to 4 (1, < 60% of the MAP2-positive cell area of controls; 2, 60–69%; 3, 70–79%; 4, ≥ 80%). Scoring was performed using a ×20 objective lens. Morphological scores were derived for eight fields/mouse (n = 3 and n = 1; Sapporo- and Oshima-inoculated mice, and a control mouse, respectively). The data are presented as a box plot. Tukey-Kramer test, **p < 0.01.

Fig. 2. Astrocytes and microglia were activated by TBEV infection in vivo. Oshima caused greater glial activation than Sapporo.

(a) Representative micrographs showing the immunohistochemistry of brain sections stained for GFAP. Arrows indicate hypertrophic cells. (b) The number of GFAP-positive cells in cerebral cortices was counted in high-power fields. (c) The relative sizes of GFAP-positive cells were measured using a fluorescent secondary antibody by ImageJ. (d) Representative micrographs showing the immunohistochemistry of brain sections stained for Iba-1. Arrows indicate the amoeboid form of microglia. (e, f) The number of Iba-1-positive cells (e) and Iba-1-positive amoeboid cells (f) in the cerebral cortices was counted in high-power fields. Data are presented as mean +SD; Tukey-Kramer test, **p < 0.01.

Fig. 3. TBEV infection induced necroptosis in the SH-SY5Y cell line rather than apoptosis or pyroptosis.

(a) The death of the SH-SY5Y cells infected with TBEV. PI-positive cells were counted at 24, 48, and 72 h. Data are presented as mean +SD; Scheffe's F test, **$p < 0.01$ and *$p < 0.05$. (b) CASP3 (a marker of apoptosis) expression was analyzed. (c) CASP1 and GSDMD (markers of pyroptosis) expression were analyzed. (d) MLKL, p-MLKL, RIP and RIP3 (markers of necroptosis) expression levels were analyzed. (e) The relative band intensities of MLKL normalized to that of the internal control were measured ($n = 4$). Data are presented as mean +SD; Steel-Dwass test, *$p < 0.05$. (f) The necroptosis inhibitor necrostatin-1s (10 or 5 mM) prevented cell death after TBEV infection. Data are presented as mean +SD; Scheffe's F test, **$p < 0.01$ and *$p < 0.05$. (g) Brains inoculated with the control or either TBEV strain were immunostained for MLKL. Arrowheads indicate MLKL-positive cells.

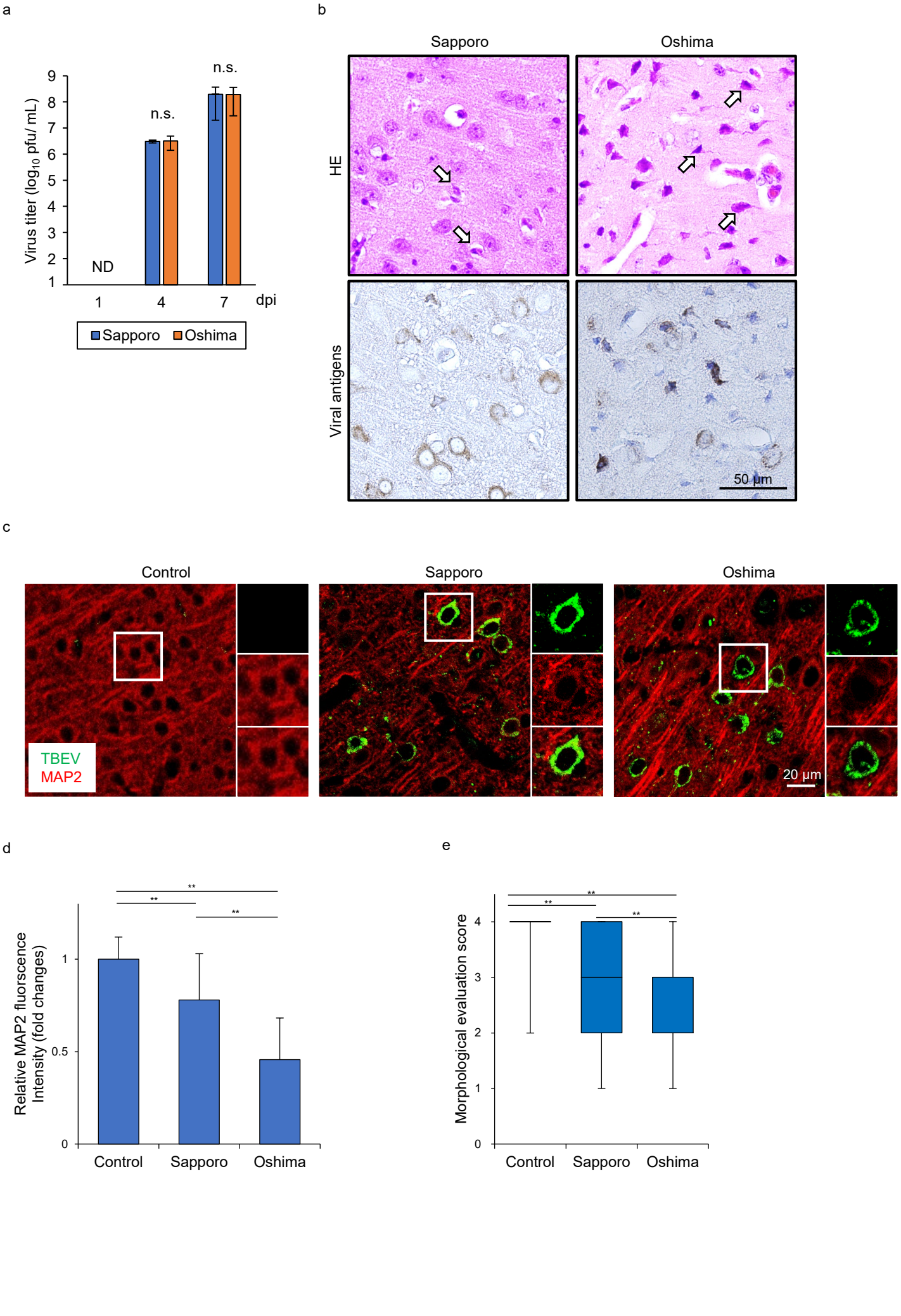
a
Virus titer (log10 pfu/ mL)
9
8
7
6
5
4
3
2
1
ND
n.s.
n.s.
1
4
7
dpi
Sapporo
Oshima
b
Sapporo
Oshima
HE
Viral antigens
50 μm
c
Control
Sapporo
Oshima
TBEV
MAP2
20 μm
d
Relative MAP2 fluorscence Intensity (fold changes)
1
0.5
0
**
**
**
Control
Sapporo
Oshima
e
Morphological evaluation score
4
3
2
1
0
**
**
**
Control
Sapporo
Oshima

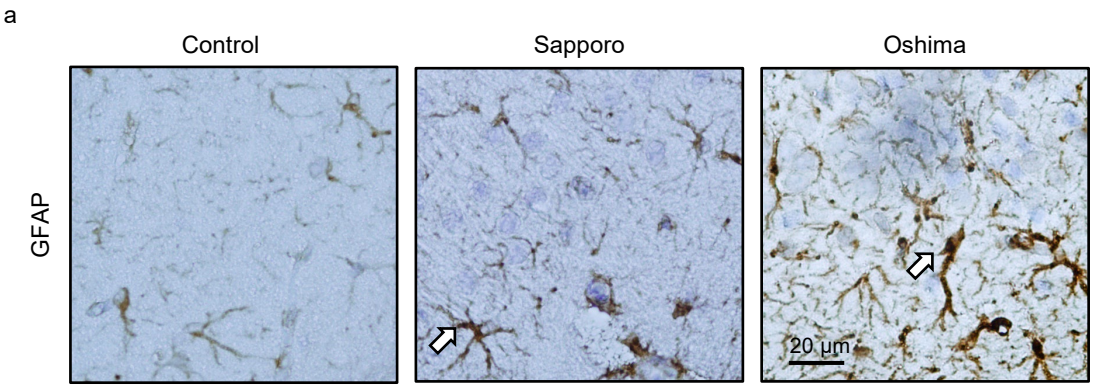
a
Control
Sapporo
Oshima
GFAP
20 μm

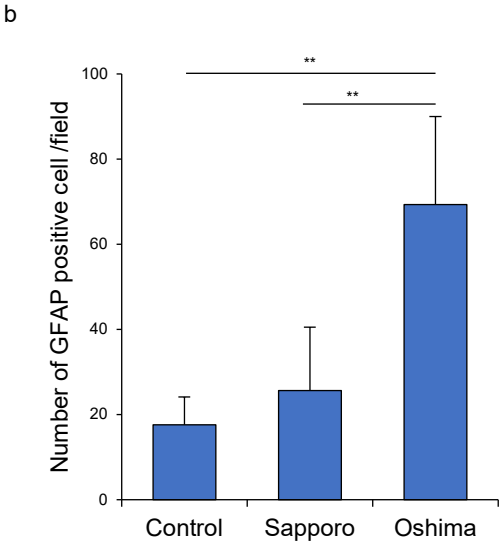
b
Number of GFAP positive cell /field
100
80
60
40
20
0
**
**
Control
Sapporo
Oshima

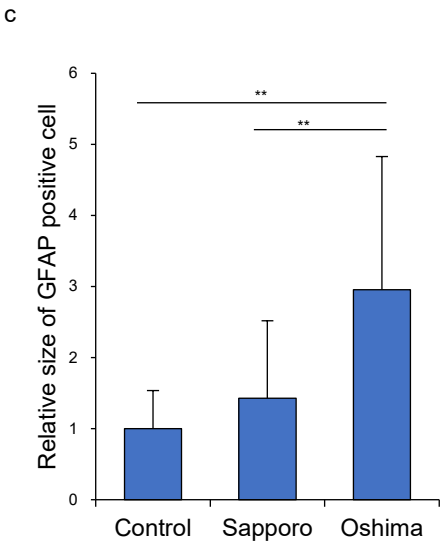
c
Relative size of GFAP positive cell
6
5
4
3
2
1
0
**
**
Control
Sapporo
Oshima

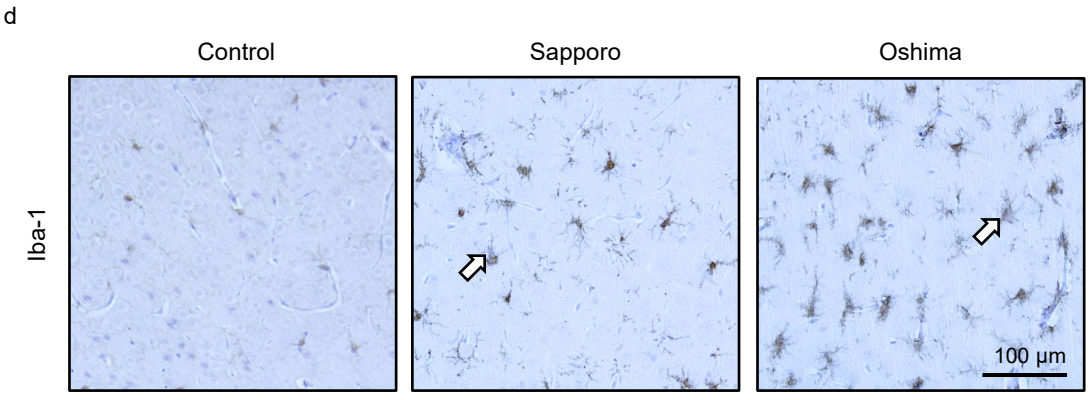
d
Control
Sapporo
Oshima
Iba-1
100 μm

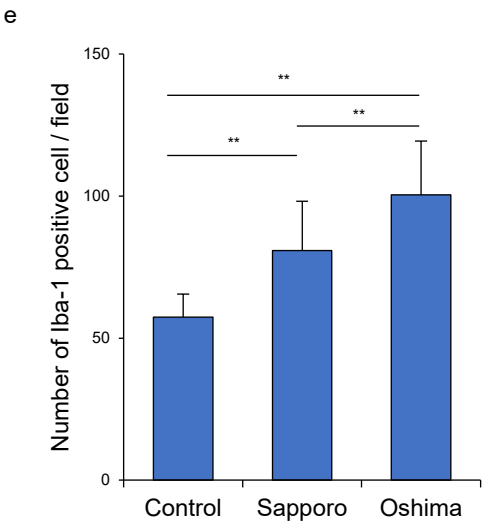
e
Number of Iba-1 positive cell / field
150
100
50
0
**
**
**
Control
Sapporo
Oshima

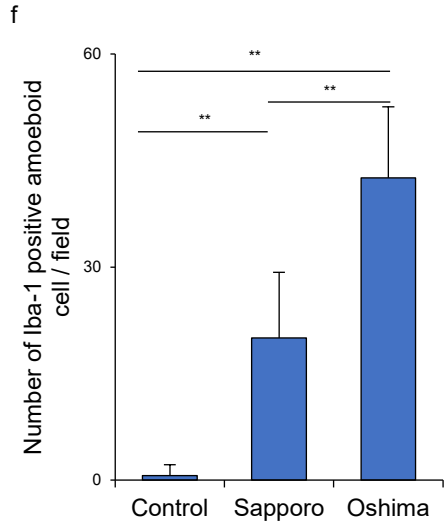
f
Number of Iba-1 positive amoeboid cell / field
60
30
0
**
**
**
Control
Sapporo
Oshima

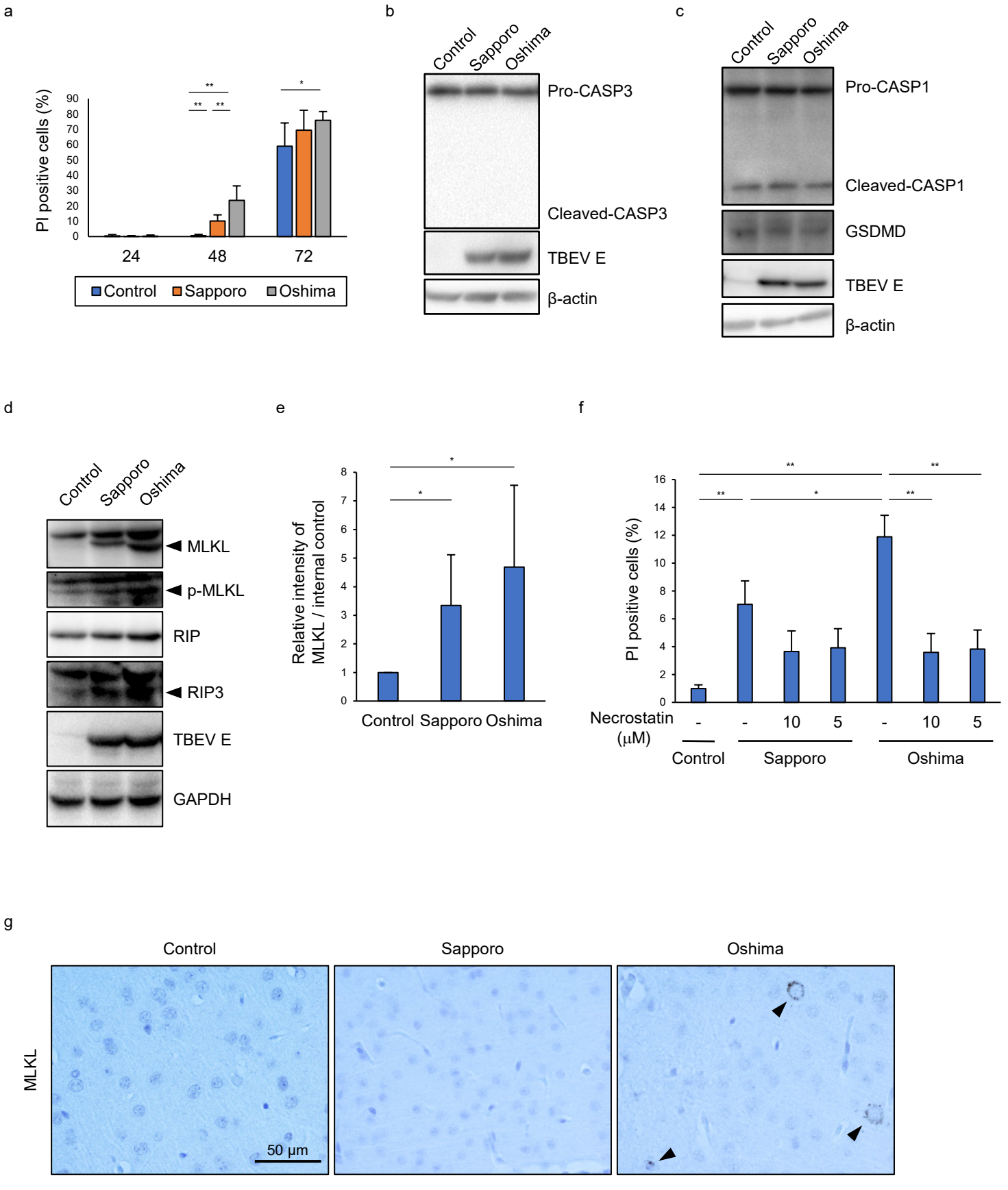
a
PI positive cells (%)
90
80
70
60
50
40
30
20
10
0
**
**
**
*
24
48
72
Control
Sapporo
Oshima
b
Control
Sapporo
Oshima
Pro-CASP3
Cleaved-CASP3
TBEV E
β-actin
c
Control
Sapporo
Oshima
Pro-CASP1
Cleaved-CASP1
GSDMD
TBEV E
β-actin
d
Control
Sapporo
Oshima
MLKL
p-MLKL
RIP
RIP3
TBEV E
GAPDH
e
Relative intensity of MLKL / internal control
8
7
6
5
4
3
2
1
0
*
*
Control
Sapporo
Oshima
f
PI positive cells (%)
16
14
12
10
8
6
4
2
0
**
**
**
*
**
Necrostatin (μM)
-
-
10
5
-
10
5
Control
Sapporo
Oshima
g
Control
Sapporo
Oshima
MLKL
50 μm